Electronic Supplementary Information

FeNC/MXene Hybrid Nanosheet as an Efficient Electrocatalyst for Oxygen Reduction Reaction

Yangyang Wen,*[a] Chang Ma, [a] Zhiting Wei [a] and Zhenxing Li *[a]

Table S1 Specific surface areas (S_{BET}) of MXene and FeNC/MXene-x determined by the nitrogen sorption isotherms.

Samples	S_{BET} / $m^2 \cdot g^{-1}$
MXene	28.1
FeNC/MXene-0.25	25.4
FeNC/MXene-0.5	26.4
FeNC/MXene-1	35.6
FeNC/MXene-2.5	34.0
FeNC/MXene-5	28.2

Table S2 Elemental compositions of MXene and FeNC/MXene-x determined by XPS.

Samples	C at.%	N at.%	Fe at.%	Ti at.%	O at.%
MXene	49.3	-	-	30.6	20.1
FeNC/MXene-0.25	44.0	2.1	2.1	14.8	37.0
FeNC/MXene-0.5	56.1	2.6	2.2	11.6	27.5
FeNC/MXene-1	57.3	2.7	2.3	9.6	28.1
FeNC/MXene-2.5	63.4	2.7	2.4	8.3	23.2
FeNC/MXene-5	70.4	1.6	3.0	5.8	19.2

Table S3 N1s core level peak analyses of FeNC/MXene-x.

N1s	Pyridinic N (398.5±0.1 eV)	Fe-Nx (399.4±0.1 eV)	Pyrrolic N (400.4±0.1 eV)	Graphitic N (401.3±0.1 eV)	Oxidized N (402.8±0.1 eV)
FeNC/MXene-0.25	28.80	11.21	21.72	28.60	9.67
FeNC/MXene-0.5	27.79	12.83	15.56	34.20	9.62
FeNC/MXene-1	23.57	14.95	12.96	35.17	13.35
FeNC/MXene-2.5	23.91	13.98	14.04	34.30	13.77
FeNC/MXene-5	25.34	9.91	17.35	33.20	14.20

Table S4 Fe2p core level peak analyses of FeNC/MXene-x.

Fe2p	Fe^{2+} $2p_{3/2}$ (711.2±0.1 eV)	Fe^{3+} $2p_{3/2}$ (713.2±0.1 eV)	Satellite (718.5±0.2 eV)	Fe^{2+} $2p_{1/2}$ (724.5±0.1 eV)	Fe^{3+} $2p_{1/2}$ (726.7±0.2 eV)	Satellite (731.5±0.1 eV)
FeNC/MXene-0.25	27.36	14.45	21.60	13.82	9.82	12.95
FeNC/MXene-0.5	26.07	15.81	20.86	16.83	11.30	9.13
FeNC/MXene-1	26.02	15.49	20.24	17.05	10.36	10.84
FeNC/MXene-2.5	24.60	17.16	20.48	14.37	11.11	12.29
FeNC/MXene-5	32.53	14.79	18.48	15.26	9.80	9.14

Table S5 Electrochemical parameters for MXene and FeNC/MXene-x catalysts.

Samples	Potential values (V)	
	Onset potential	Half-wave potential
MXene	0.71	0.529
FeNC/MXene-0.25	0.95	0.743
FeNC/MXene-0.5	0.98	0.788
FeNC/MXene-1	1.00	0.814
FeNC/MXene-2.5	1.00	0.793
FeNC/MXene-5	0.99	0.771
Pt/C	1.03	0.789

Table S6 Comparison of electrocatalytic ORR performances between this work and other works in alkaline medium.

Catalysts	Onset potential (V vs. RHE)	Half-wave potential (V vs. RHE)	References
FeNC/MXene-1	1.00	0.814	This work
$FePc/Ti_3C_2T_x$	0.97	0.89	1
Fe-N-C/rGO	0.94	0.81	2
Fe-N/C-800	0.97	0.82	3
Fe-N-graphene	1.01	0.81	4
Fe/C/N	0.94	0.83	5
N-doped Fe/Fe_3C@graphitic layer/CNT	-	0.715	6

Table S7 Comparison of ORR stability between this work and other works.

Catalysts	Stability	References
FeNC/MXene-1	97.4 % retention over 20000s	This work
$FePc/Ti_3C_2T_x$	74 % retention over 5000s	1
Fe-N-C/rGO	92.8 % retention over 12000s	2
3D microporous Fe-N-C	94.5 % retention over 100000s	7
FeN/C	88.8 % retention over 20000s	8
Porous Fe-N-C	81 % retention over 80000s	9
FexN/NGA hydrid	91 % retention over 20000s	10

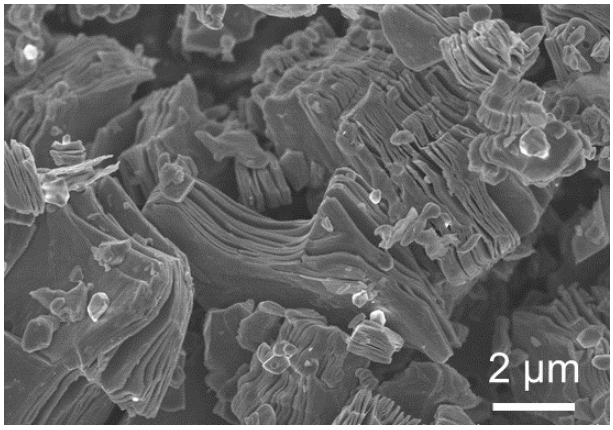

Fig. S1 SEM image of the multilayered $Ti_3C_2T_x$ powder.

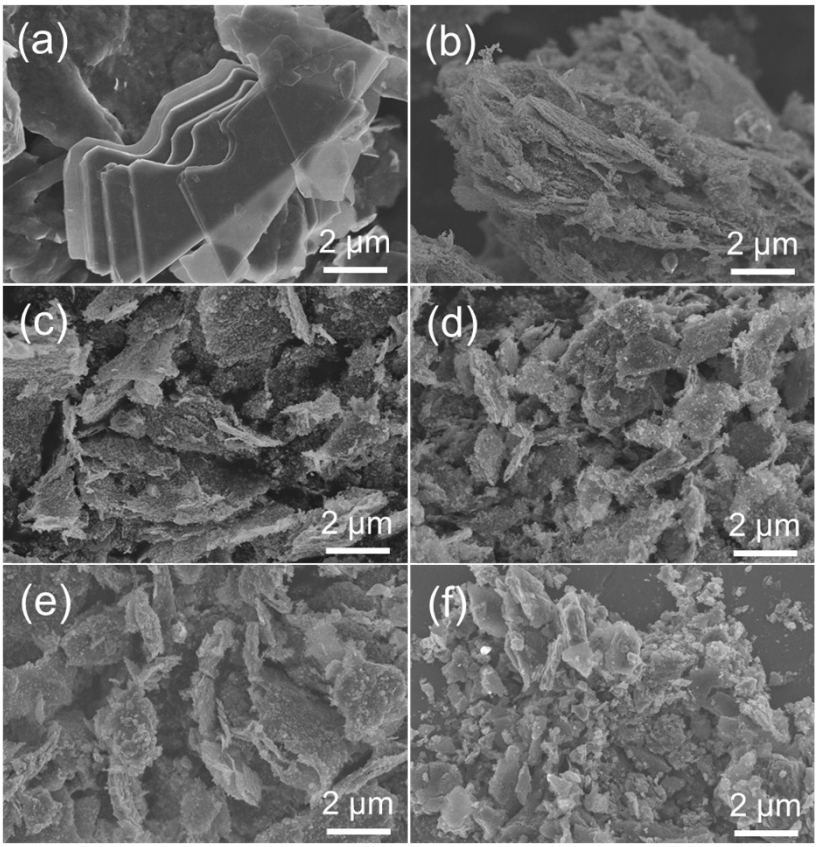

Fig. S2 SEM images of the pritine $Ti_3C_2T_x$ MXene (a), FeNC/MXene-0.25 (b), FeNC/MXene-0.5 (c), FeNC/MXene-1 (d), FeNC/MXene-2.5 (e), and FeNC/MXene-5 (f) at low magnification.

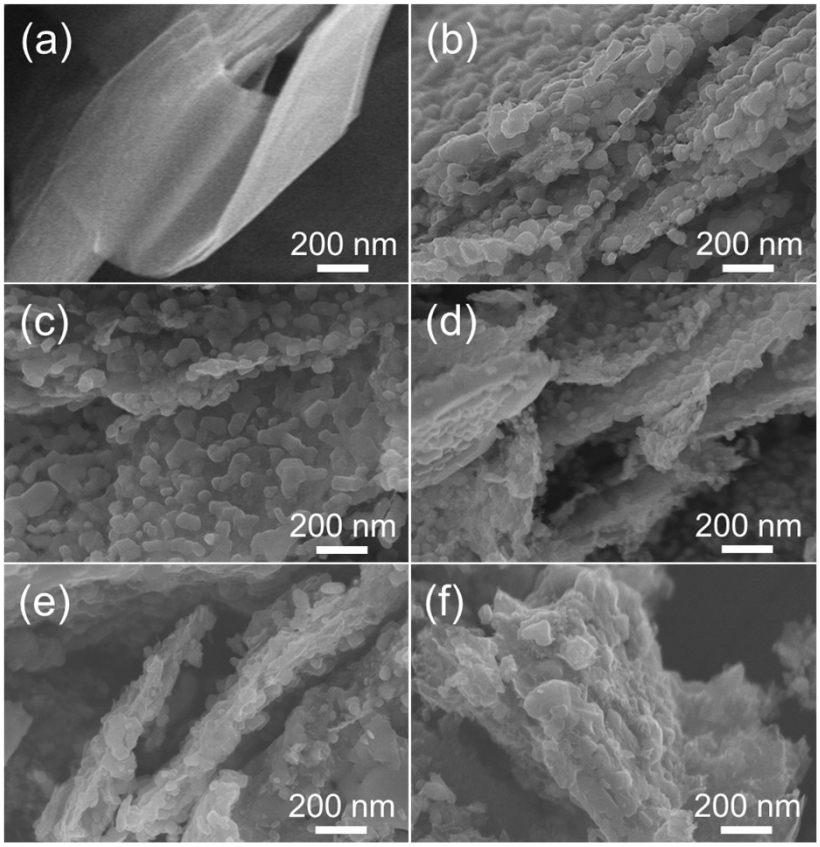

Fig. S3 SEM images of the pritine $Ti_3C_2T_x$ MXene (a), FeNC/MXene-0.25 (b), FeNC/MXene-0.5 (c), FeNC/MXene-1 (d), FeNC/MXene-2.5 (e), and FeNC/MXene-5 (f) at high magnification.

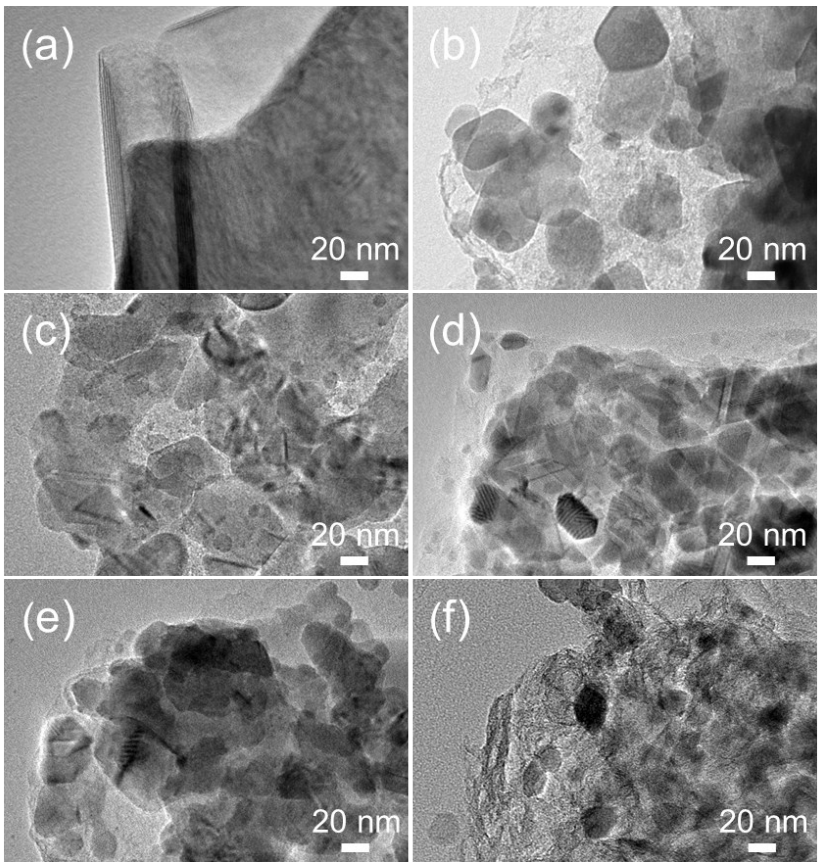

Fig. S4 TEM images of the pritine $Ti_3C_2T_x$ MXene (a), FeNC/MXene-0.25 (b), FeNC/MXene-0.5 (c), FeNC/MXene-1 (d), FeNC/MXene-2.5 (e), and FeNC/MXene-5 (f).

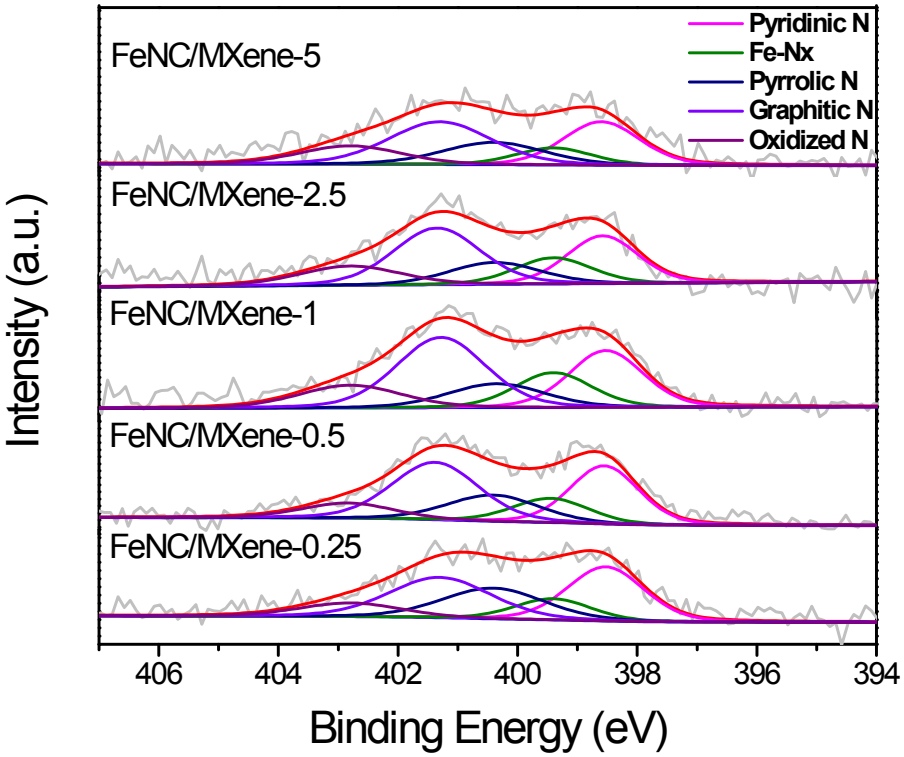

Fig. S5 XPS N1s binding energy regions of FeNC/MXene-x.

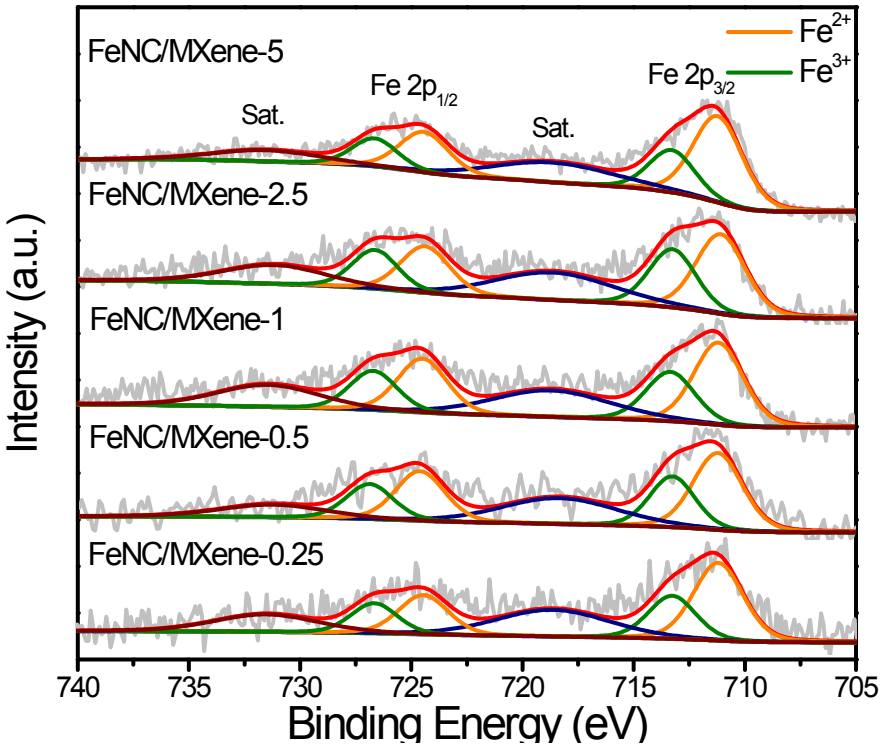

Fig. S6 XPS Fe2p binding energy regions of FeNC/MXene-x.

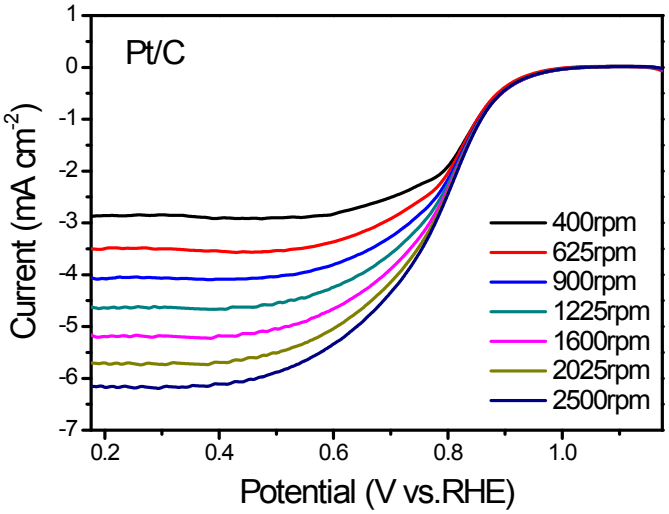

Fig. S7 LSV curves of the Pt/C catalyst in O_2-saturated 0.1 M KOH solution at 50 mV·s^{-1} with different rotating rates.

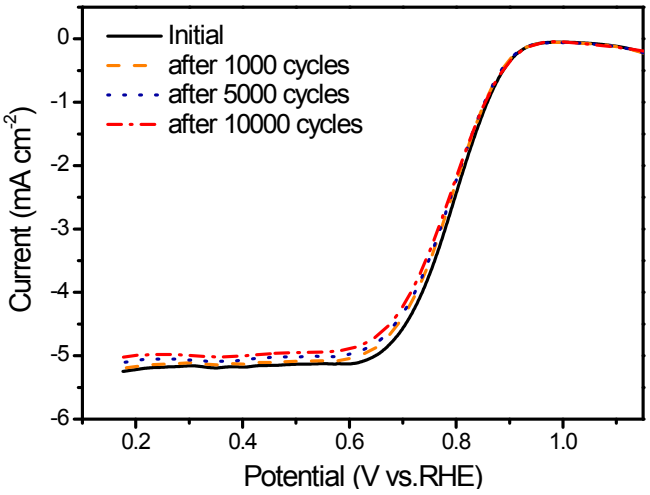

Fig. S8 LSV plots of FeNC/MXene-1 catalyst before and after the durability test over 10000 cycles at 1600 rpm.

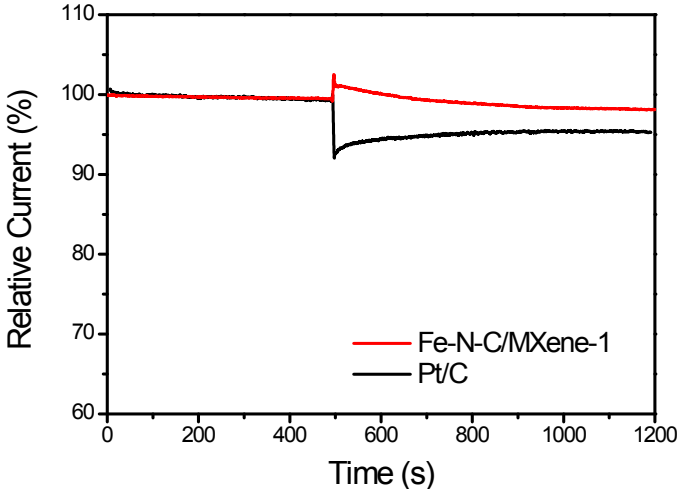

Fig. S9 Chronoamperometric responses of FeNC/MXene-1 and the Pt/C catalyst at 0.275 V in O_2-

saturated 0.1 M KOH solution followed by addition of 3 M methanol.

References

1. Z. Li, Z. Zhuang, F. Lv, H. Zhu, L. Zhou, M. Luo, J. Zhu, Z. Lang, S. Feng, W. Chen, L. Mai and S. Guo, *Adv. Mater.*, 2018, **30**, 1803220.
2. C. Zhang, J. Liu, Y. Ye, Z. Aslam, R. Brydson and C. Liang, *ACS Appl. Mater. Inter.*, 2018, **10**, 2423-2429.
3. W. Niu, L. Li, X. Liu, N. Wang, J. Liu, W. Zhou, Z. Tang and S. Chen, *J. Am. Chem. Soc.*, 2015, **137**, 5555-5562.
4. C. He, J. J. Zhang and P. K. Shen, *J. Mater. Chem. A*, 2014, **2**, 3231-3236.
5. Y. Zhao, K. Kamiya, K. Hashimoto and S. Nakanishi, *J. Phys. Chem. C*, 2015, **119**, 2583-2588.
6. J. S. Li, S. L. Li, Y. J. Tang, M. Han, Z. H. Dai, J. C. Bao and Y. Q. Lan, *Chem. Comm.*, 2015, **51**, 2710-2713.
7. W. Wang, W. Chen, P. Miao, J. Luo, Z. Wei and S. Chen, *ACS Catal.*, 2017, **7**, 6144-6149.
8. J. Cao, X. Jia, M. Guo, Y. Du, J. Xu and Z. Chen, *Sustain. Energ. Fuels*, 2018, **2**, 169-174.
9. Q. Zuo, P. Zhao, W. Luo and G. Cheng, *Nanoscale*, 2016, **8**, 14271-14277.
10. H. Yin, C. Zhang, F. Liu and Y. Hou, *Adv. Funct. Mater.*, 2014, **24**, 2930-2937.